EDDIES AND SST FRONTAL VARIABILITY IN EASTERN BOUNDARY CURRENTS

Yeping Yuan (yyping@uga.edu) and **Renato M. Castelao*** (castelao@uga.edu)
Dept. of Marine Sciences, University of Georgia, U.S.A.

Abstract:

The majority of mesoscale eddies in the ocean have been shown to be highly nonlinear. This is important, because as such they are capable of trapping water in their interior as they propagate. By transporting momentum, heat, mass and the chemical constituents of seawater, they can contribute to water mass distributions and ocean biology. Here, we use satellite observations of sea surface height and sea surface temperature to specifically focus on the influence of eddies on the distribution of fronts in Eastern Boundary Currents. Previous studies have shown that the area near the coast with high frontal activity broadens during the upwelling season, and several mechanisms have been suggested to explain that phenomena. Satellite observations and idealized numerical model simulations are used to demonstrate that nonlinear eddies play an important role in that process. Model simulations are further used to investigate the influence of the coupling between eddies and winds on upwelling and SST frontal variability in Eastern Boundary Currents.

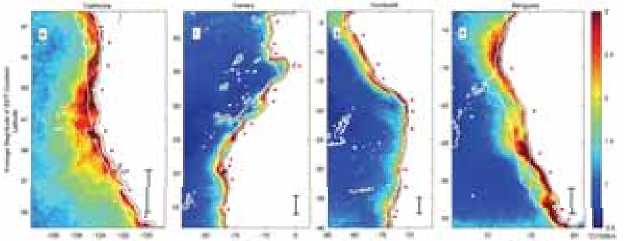

Fig 1. Average sea surface temperature (SST) gradient magnitude (°C per 100 km) from 2003 to 2009 in all Eastern Boundary Current Systems (EBCS; the California, Canary, Humboldt, and Benguela Current Systems). The spatial distributions of SST gradients share similar patterns in different regions. The dominant pattern is that strong SST gradients are generally observed along the coast, decreasing with distance from the coast. This leads to a consistent distribution of average frontal probabilities, which are also enhanced near the coast, gradually decreasing offshore. An offshore migration of the region of high SST gradients (frontal probability) is generally observed, with high SST gradients first appearing close to the coast during spring, moving offshore during summer and fall (e.g., *Wang et al., 2015*).

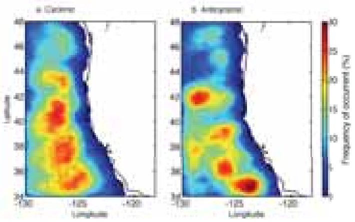

Fig 2. Frequency of occurrence (percentage of time that eddies are observed at a given location) of (a) cyclonic and (b) anticyclonic eddies with lifetime > 4 weeks in California Current System (CCS) from 1992 to 2012.

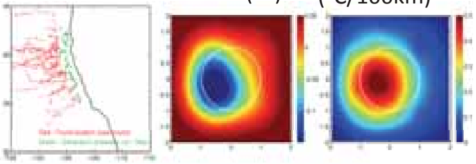

a. Trajectories

b. SST (°C)

c. SST gradient (°C/100km)

Fig 3. Trajectories of cyclonic eddies in the CCS that were generated within 200 km from the coast (red dots) and then propagated offshore. Their generation locations are shown by the green circles (a). Composite averages of eddy SST (b) and SST gradient (c) overlaid by one eddy radius for eddies shown in panel (a), red dots. The x and y coordinates of the composite averages are normalized by the eddy radius, defined in *Chelton et al., 2011*. Eddies of either polarity are associated with enhanced SST gradients in their interior.

Eddy-induced SST gradient

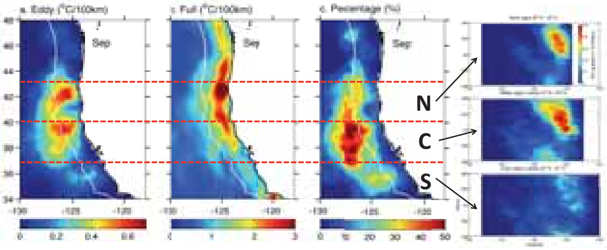

Fig 4. Average SST gradient due to eddies that were generated within 200 km from the coast and then propagated offshore (Fig. 3a red dots) in September (a). Full SST gradients are shown in (b), while the ratios between eddy-induced and full SST gradients are shown in (c). The white contours show the offshore distance of 200 km. The seasonal cycles of meridional averages of the eddy–induced SST gradient in a northern (40°N – 43°N), central (37°N – 40°N) and southern (34°N – 37°N) sectors are shown in (d). High SST gradients are generally observed along the coast within 200 km offshore, while localized high eddy-induced SST gradients are observed near 40°N and 39°N, extending farther offshore. The eddy-induced SST gradient contributes up to 50% of the full SST gradient in September in regions farther from 200 km from the coast. The high eddy-induced SST gradients in the northern and central sectors generally initiate around July, after which they propagate offshore. Values peak in fall, decreasing in early winter. Eddy-induced SST gradients are substantially weaker in the southern region.

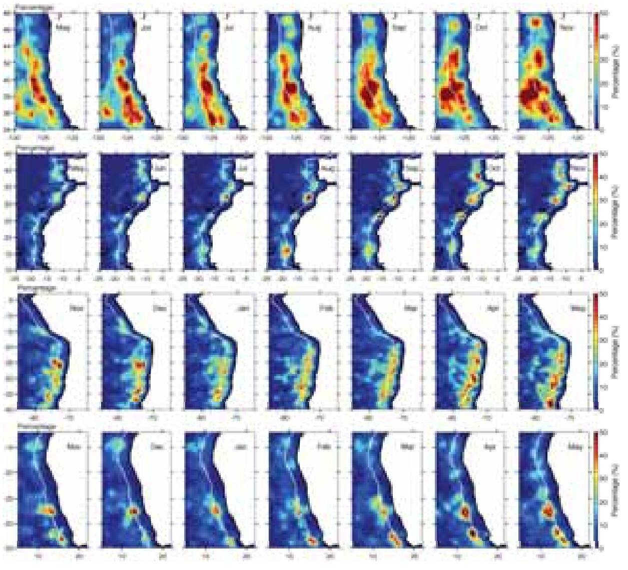

Fig 5. Monthly evolution of the ratio between eddy-induced and full SST gradients in all EBCS during the upwelling season. Only eddies that were generated within 300 km from the coast and then propagated offshore were used in the calculation. Eddies can contribute up to 50% of the full SST gradients at ~300 km offshore.

Idealized model results

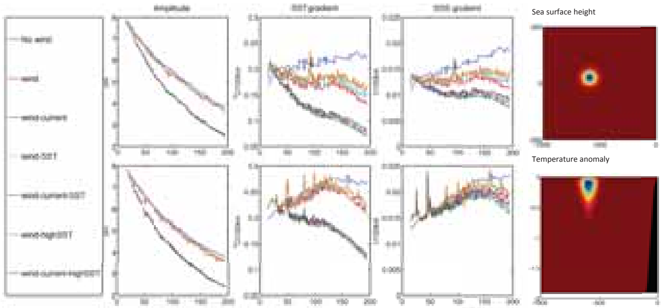

Fig 6. Idealized numerical model of typical cyclone (top three panels) and anti-cyclone (bottom three panels) in CCS (-+8cm amplitude; 80km radius) under steady upwelling favorable winds with different wind coupling conditions. Upwelling favorable winds lead to decreases in amplitude and SST and SSS gradients. The influence of the wind is strongest with wind-current coupling, while the wind-SST coupling only slightly modifies the surface gradients.

Conclusions

1. Eddy-induced SST gradient contributes up to 50% of the full SST gradient in EBCS during upwelling seasons;
2. Our result suggests that eddy westward propagation is one possible mechanism for broadening the high SST gradient band, which relates to the high frontal activity broaden;
3. Idealized model shows that upwelling favorable wind leads to decreases in eddy amplitude and SST and SSS gradients.

Reference:

Chelton, D., M. Schlax, and R. Samelson (2011), Global observations of nonlinear mesoscale eddies, Prog. Oceanogr., 91, 167–216.
Wang, Y., R. M. Castelao, and Y. Yuan (2015), Seasonal variability of alongshore winds and sea surface temperature fronts in Eastern Boundary Current Systems, J. Geophys. Res. Oceans, 120, 2385–2400

Acknowledgement:

The authors thank Physical Oceanography Distributed Active Archive Center (PO.DAAC) for providing SST data at: http://podaac.jpl.nasa.gov. The global eddy dataset was developed and made freely available by D. Chelton and M. Schlax at: http://cioss.coas.oregonstate.edu/eddies/. This work was funded by NASA Grant NNX13AD80G.